Aerospace **2014**, *1*, 67-96; doi:10.3390/aerospace1020067

OPEN ACCESS

aerospace

ISSN 2226-4310

www.mdpi.com/journal/aerospace

Review

Reforming Technologies to Improve the Performance of Combustion Systems

Hashim Hassan and Bhupendra Khandelwal *

Mechanical Engneering Department, The University of Sheffield, Sheffield, S1 3JD, UK;
E-Mail: hashim_hassan@live.com

* Author to whom correspondence should be addressed; E-Mail: bhupendra.khandelwal@gmail.com;
Tel.: +44-74111-08151.

Received: 7 February 2014; in revised form: 30 June 2014 / Accepted: 7 July 2014 /
Published: 4 September 2014

Abstract: A large number of theoretical and experimental studies have shown that the performance of kerosene combustion increases significantly if combustion is being assisted by the addition of hydrogen to the fuel/air mixture during the combustion process. It reduces the amount of CO, CO_2 and NO_x emissions, while increasing the flame stability limits. It also helps in bruning fuel/air mixtures at much leaner equivalence ratios. The same principle could be applied to gain benefits in gas turbine combustors. Hydrogen for this purpose could be produced by the reforming of hydrocarbon fuels using a reformer module. This paper presents key hydrogen reforming technologies which, by implementation in gas turbine combustors, hold potential for improving both their performance and service life.

Keywords: kerosene reforming; gas turbine combustor; novel combustion technologies; hydrogen assisted combustion

---

1. Introduction

Gas turbine engines are widely used in the aerospace, marine and energy industries due to their performance, and their reliable and robust design. Recently, with environmental concerns becoming more prevalent, a significant amount of attention has been drawn to the emissions of gas turbine engine combustors, particularly for those used on aircraft. These emissions consist mostly of exhaust gases including carbon dioxide (CO_2), carbon monoxide (CO), un-burnt hydrocarbons (UHCs) and oxides of nitrogen (NO_x), and have been shown to have pernicious effects on human health and as well as the earth's environment. With gas turbine engines finding wider uses resulting from factors such as an increase in air travel and power generation, an increase in these exhaust gases will surely have deleterious effects, and may result in tighter restrictions being placed on gas turbine performance characteristics. Thus, it is imperative to reduce these emissions by making modifications to existing gas turbine combustion systems [1–7].

Hydrogen assisted combustion involves the addition of hydrogen (or hydrogen rich gases) to the fuel–air mixture in the combustion chamber of gas turbine engines. Introducing hydrogen in this manner to the gases in the combustor has been shown to reduce the amount of harmful emissions from the combustor and also to improve the overall combustion performance of the engine [3]. Various studies, such as those by Juste [1] and Frenillot *et al.* [2], have examined both quantitatively and qualitatively the improvement in combustor performance in terms of reductions in emissions. The specific heat of hydrogen is approximately 3 times that of other hydrocarbon fuels. Hydrogen has wider flame stability limits and laminar flame speeds when used for combustion and a lower emissivity which means that the structure of the engine sustains lower thermal stresses and less fatigue, leading to a longer service life.

Frenillot *et al.* [2] showed that with increasing the amount of hydrogen in the combustion reaction, the amount of NO_x generated decreases. This is due to the fact that hydrogen has much higher flame stability limits as compared to kerosene. This would help in burning the air/fuel mixtures at a much leaner equivalence ratios, which would eventually reduce overall emissions. Increase in the flame stability limits will also increase the flame stability limits of a gas turbine combustor and altitude relight could become much easier [3].

The hydrogen produced for the purpose of acting as an additive for gas turbine combustion systems, is commonly produced together with CO, and the resulting gaseous mixture is referred to as synthesis gas or "syngas" [3]. There are several processes by which syngas is produced, a wide range of them have been discussed in this paper. The various reactor designs, fuel delivery systems and catalysts and porous media have also been systematically analysed in order to contribute to the understanding of the processes which hold the potential for improving the performance of gas turbine combustion systems.

The purpose of this paper is to present a review of key technologies in the area of hydrogen reforming, with an emphasis on those which could be implemented in the future in aircraft gas turbine engines, as well as an identification of the gaps present in the current knowledge and understanding of the principles behind these technologies. By identifying these gaps, future research can be dictated such that a complete understanding of the combustion characteristics, as well as the physical integration of a hydrogen reformer module in aircraft engines, can be made and the performance of these engines can improved.

2. Reforming Processes

2.1. Thermal or Non-Catalytic Partial Oxidation (TPOX)

Thermal or Non-Catalytic Partial Oxidation (TPOX) is an exothermic reaction and is usually performed without the use of a catalyst or an external heat source. The low hydrogen yield and the production of soot are, however, the major drawbacks of this process. The TPOX chemical equation for methane is shown below.

$$2CH_4 + O_2 \rightarrow 2CO + 4H_2;\ \Delta H < 0 \tag{1}$$

Several studies have aimed at investigating the production of hydrogen (syngas) using TPOX [8]. The use of inert porous media is common in such experiments due to the fact that their presence has been shown to improve the reaction characteristics [8].

Al-Hamamre *et al.* [8] investigated the production of hydrogen by TPOX of hydrocarbon fuels in an inert porous media based reformer. The aim was to determine the practical operating conditions of the reforming process and also to analyze the effects of varying parameters such as air pre-heating temperature, thermal load and air ratio. The fuel used was methane, and two different reformer modules were designed for the experimental procedures. The differences in the two reformers arose from the choice of materials used for the porous media base in their reaction chambers. The first was an Al_2O_3 static mixer structure and the second was SiC foam (10 ppi). The experimental setup is shown in Figure 1 and the reformer module is shown in Figure 2.

Figure 1. Experimental setup used by Al-Hamamre *et al.* [8].

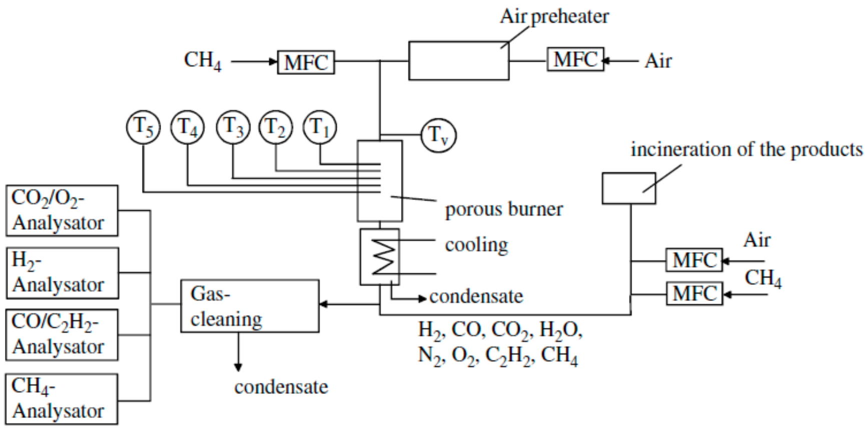

Figure 2. Reformer module used by Al-Hamamre *et al.* [8].

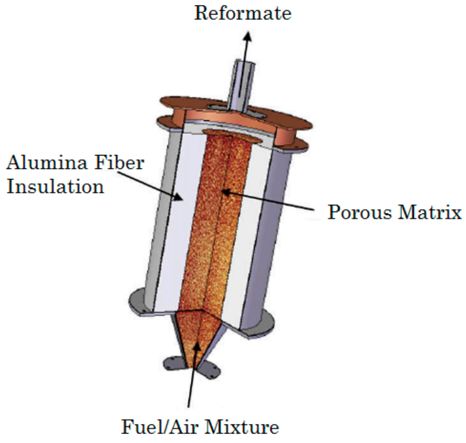

Using the setup shown in Figure 2 experiments were performed with different pre-heating temperatures, air ratios and thermal loads. Temperature measurements were taken at the center axis at the reformer inlet and outlet, and reformate samples were taken at various distances in the reformer. Al-Hamamre *et al.* concluded in their study that an equivalence ratio down to 0.4 was the practical limit to perform TPOX of methane. The air pre-heating temperature has no significant effect on the reformation process. However, it did affect the soot point such that the SiC foam showed a lower soot point of 0.42 at an air pre-heating temperature of 700 °C compared to 0.45 for the Al_2O_3 static mixer.

Loukou *et al.* [9] conducted a study on hydrogen production and soot particulate emissions from rich combustion of methane in an inert porous media based reactor. Two different porous matrices were used; SiSiC, which has an open foam structure, and a packed bed of pure Al_2O_3 in the form of cylindrical rings. A schematic of the reformer is shown in Figure 3. The module has a conical entry to ensure flame stabilization and a constant cylindrical cross-section for adequate residence times and to ensure the completion of slow reactions. The reactants are heated upstream of the reformer, and the effects of pre-heating were also investigated. Soot particle size distributions were measured in the exhaust gases using a Scanning Mobility Particle Sizer (SMPS).

Figure 3. Reformer device for the experimental procedures [9].

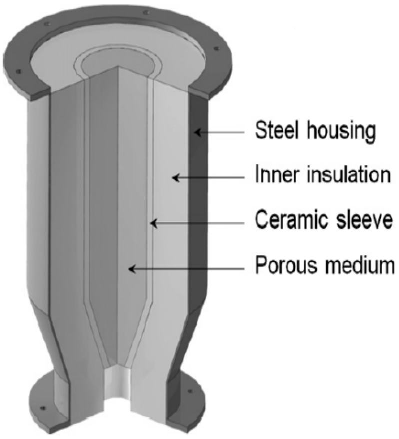

Loukou *et al.* [9] showed that in the case of the SiSiC matrix the flame stabilizes within the conical section of the reformer for a wider range of mass fluxes, especially at higher equivalence ratios. This is due to the superior thermal properties of the SiSiC foam which result in higher rates of internal heat recuperation. Since flame stabilization occurs in a more downstream position, the longer residence time allows for the evolution of slow reforming reactions and hence results in a higher concentration of H_2 and CO in the syngas produced. The SiSiC foam also produced significantly less soot in terms of particle size and concentration.

2.2. Catalytic Partial Oxidation (CPOX)

Catalytic Partial Oxidation (CPOX) requires the use of a catalyst, and the fuel typically used for the purpose of producing syngas through this process is methane. The key reaction, which is exothermic, is represented by the equation:

$$CH_4 + \left(\frac{1}{2}\right)O_2 \rightarrow CO + 2H_2;\ \Delta H < 0 \tag{2}$$

The complete partial oxidation of methane constitutes a system of equations and is shown in Table 1.

Various studies have aimed at investigating the characteristics of catalytic partial oxidation, some of them have been discussed in this paper with an aim to be used in a gas turbine engine.

Table 1. Complete equation system for POX of methane [10].

Chemical Equation	Number
$CH_4 + 2O_2 \rightarrow CO_2 + 2H_2O$	(i)
$CH_4 + 0.5O_2 \rightarrow CO + 2H_2$	(ii)
$CH_4 + O_2 \rightarrow CO_2 + 2H_2$	(iii)
$CO + H_2O \leftrightarrow CO_2 + H_2$	(iv)
$CH_4 + H_2O \leftrightarrow CO + 3H_2$	(v)
$CH_4 + CO_2 \leftrightarrow 2CO + 2H_2$	(vi)
$CO + H_2 \leftrightarrow C + H_2O$	(vii)
$CH_4 \leftrightarrow C + 4H_2$	(viii)
$2CO \leftrightarrow CO_2 + C$	(ix)
$CO + 0.5O_2 \rightarrow CO_2$	(x)
$H_2 + 0.5O_2 \rightarrow H_2O$	(xi)

Korup *et al.* [11] conducted a study on the catalytic partial oxidation of methane on platinum using spatially resolved profiles, Raman spectroscopy, electron microscopy and micro-kinetic modeling. The catalyst used was a Pt-coated foam monolith, and is shown in Figure 4. There were tow distinct reactions zones in the reactor: a fast exothermic oxidation reaction at the reactor entrance and a comparatively slow endothermic reforming chemistry. Using Raman spectroscopy and electron microscopy, it was found that the transportation of the Pt catalyst and the formation of carbonaceous deposits, which blocked the majority of active sites, were responsible for the position of the mechanistic change. The measured reaction profiles were compared with predicted results from two numerical micro-kinetic models. Although the results were in agreement with the oxygen profiles, the branching ratio between the partial oxidation and complete oxidation reaction was different for the two models. Carbon formation, which was not incorporated into the models was responsible for the experimentally observed change in reaction rates. The results for the H_2/CO production, for the models developed by Deutschmann *et al.* [12–14] and the one developed by Mhadeshwar *et al.* [15], Hauptmann *et al.* [16] are shown in Figure 5 below. The hydrogen production by this method is about 20% by mass fraction, which could work to be used on a gas turbine combustor.

Figure 4. Platinum coated monolithic catalyst [11].

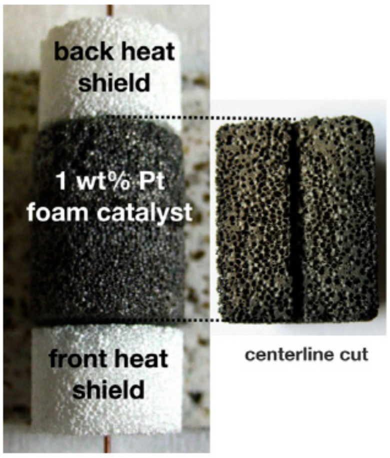

Figure 5. Mole fractions of H_2 and CO vs axial position, with a gas feed of $CH_4/O_2/Ar$ = 592/296/1112 mln/min and $CH_4/O_2/Ar$ = 1184/592/2224 mln/min respectively [11].

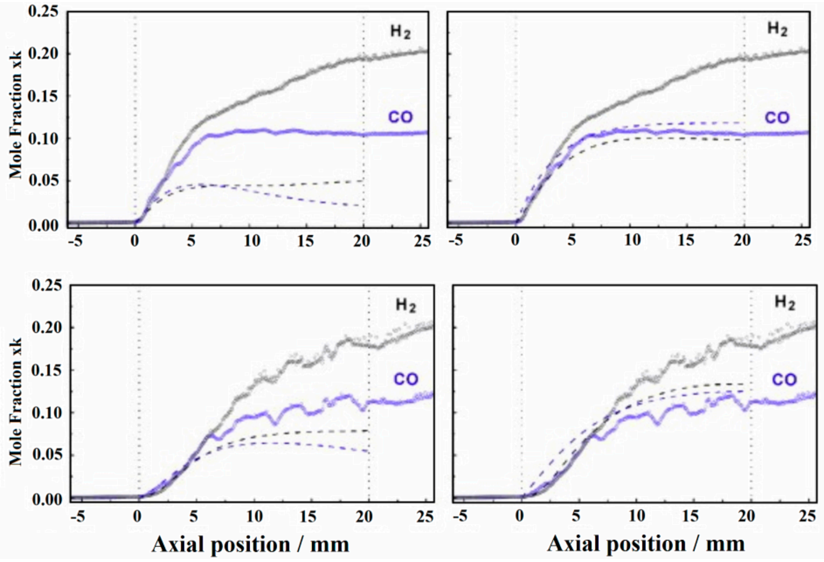

Khine *et al.* [17] studied syngas production through catalytic partial oxidation of methane over lanthanum chromite ($LaACrO_3$) and lanthanum ferrite ($LaAFeO_3$) perovskites with A-site doping of Ba, Ca, Mg and Sr, for fuel cell applications. The catalysts were prepared by solid state reactions. The graphs for the catalytic activity for the two catalyst types are shown in Figure 6. It was found that A-site doping generally increased the mobility of lattice oxygen ions and therefore decreased the temperature of H_2 and CO production as compared to undoped $LaCrO_3$ and $LaFeO_3$. Both catalysts showed stable performance during the generation-regeneration cycles, but $LaFeO_3$ showed slightly better performance. $(La_{0.75}Sr_{0.25})$ FeO_3 showed the best performance (65% CH_4 conversion, 10% H_2 and 2.8% CO production at 850 °C with 100% H_2 selectivity), and is a promising atomic oxygen source for syngas production via catalytic POX of methane.

Figure 6. Catalytic activity of partial oxidation of 5% CH_4 at 850 °C and GHSV = 750 h^{-1} [17].

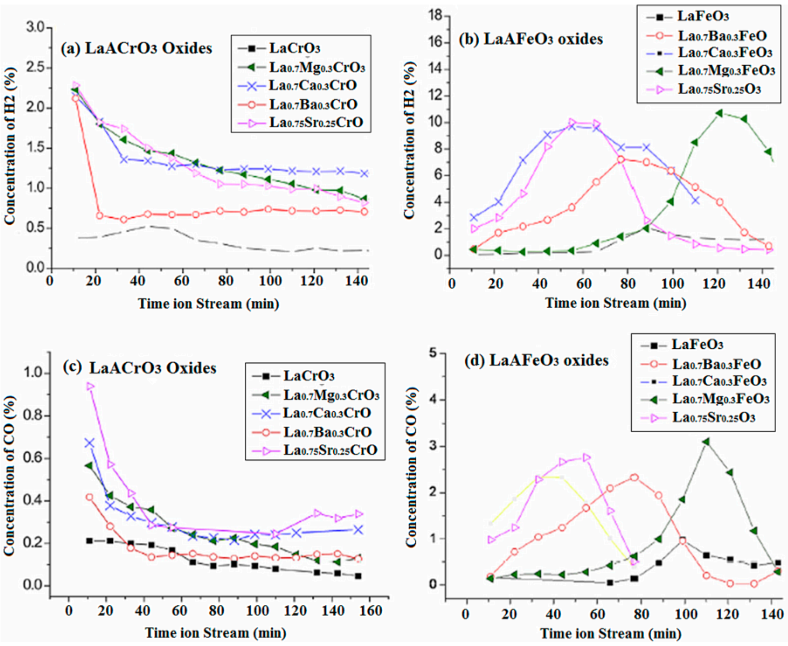

Huang *et al.* [18] conducted a study on the catalytic partial oxidation of n-butanol over LDH derived Ni-based catalysts. The catalysts were prepared using co-precipitation. CPOX was performed using a fixed-bed reactor and gas chromatography was used to analyze the products. Experimental results indicated that the hydrogen production can be increased from 3.76 to 4.01 if O_2 to butanol ratio is increased from 1.5 to 2.0, and the temperature is kept at 700 °C. The catalysts were proven effective for use in CPOX reactions, and the $Ni_{0.35}Mg_{2.65}Al_{0.5}Fe_{0.5}O_{4.5\pm\delta}$ catalyst was found to give suitable performance, producing 4.03 moles of H_2 per mole of butanol at 700°C, and an O_2 to butanol ratio of 2.0.

The CPOX of methane rich mixtures in non-adiabatic monolith reactors was investigated in study by Navalho *et al.* [19]. A rhodium based catalyst was used for the experiments. A unidimensional heterogeneous mathematical model was used for adiabatic and non-adiabatic honeycomb monolith reactors. The influence of radiative heat loss on the performance of the non-adiabatic reactor was also investigated by varying the fuel flow rate, air to fuel ratio and fuel composition. It was shown that the radiative heat loss can change the heat release as compared to the adiabatic reactor, and make the reaction more exothermic. This proved the lower importance of endothermic reforming reactions in the overall process. Generally, the non-adiabatic reactor showed a lower maximum catalyst temperature during the process, as compared to the adiabatic reactor. This is important in order to prevent catalyst deactivation during prolonged use of the reactor.

Donazzi *et al.* [20] investigated the influence of pressure on autothermal CPOX of methane and propane. The experiments were conducted with pressures varying between 1 and 4 bar, and an adiabatic reactor was used. The catalyst used was 2 weight-percent Rhodium/α-Al_2O_3 supported on a 400 cpsi cordierite honeycomb. Donazzi *et al.* [20] used spatially resolved temperature and composition profiles, together with a numerical model of the reactor which included detailed descriptions of gas phase and surface kinetics as well as homogeneous and heterogeneous reaction chemsitry. It was found that below a value of 4 bar, pressure caused an increase in the outlet temperature. At the inlet of the catalyst, pressure had a minimal effect on the reaction kinetics. Furthermore, no change was recorded in the hot spot temperature, which is very important for the durable and stable operation of a CPOX reactor. Heterogeneous, instead of homogeneous reactions, were affected thermodynamically by pressure. In the final part of the catalyst, pressure increase causes an increase in the outlet temperature. In the first part, pressure has no effect on temperature or concentration profiles. Homogeneous reaction do not take place during the CPOX of methane, but during the propane CPOX, pressure promotes a cracking reaction which leads to the production of methane and C^{2+} species.

A study by Chen [21] looked at CO_2 conversion for syngas production during CPOX of methane. CPOX of methane is essentially a combination of methane combustion, steam reforming and dry reforming. The CO_2 produced from combustion is used to produce syngas in methane combustion. Chen [21] conducted a numerical study where carbon dioxide is added to the feed gas for CPOX and the reaction is triggered. It was found that CO_2 impedes steam reforming and enhances dry reforming. Generally, increasing CO_2 decreases H_2 but increases CO formation. A maximum conversion was obtained at a carbon dioxide to oxygen ratio of 0.2, and with an increasing O/C ratio, the CO_2 conversion decreases. This is shown in Figure 7a,b.

Figure 7. (**a**) Hydrogen yield *vs.* O/C ratio; (**b**) H_2/CO ratio *vs.* O/C ratio [21].

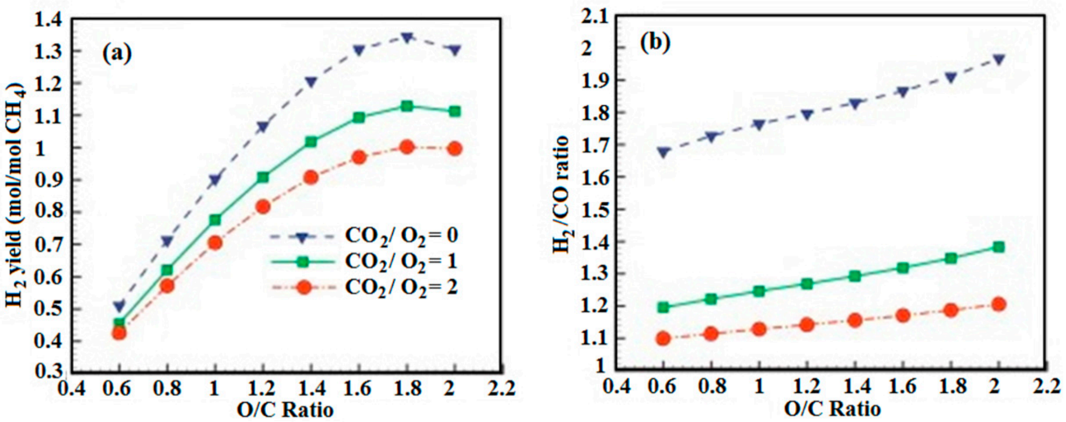

Plasma-assisted gliding arc reactor was used to model the CPOX of methane to syngas by Rafiq *et al.* [22]. A 2-D heterogeneous plug-flow radial dispersion with no gradients inside the catalyst pellet was used. Temperature, reactant conversion, hydrogen yield and CO yield, showed results which were similar both for simulation and the experimental data. The numerical model was extended to predict results for increasing the GHSV and the reactor energy density (RED). It was found that an increase in the GHSV caused a decrease in the reactant conversion and H_2 and CO yields. The peak temperature also increased. An increase in the RED resulted in an increase in the CH_4, H_2O and CO_2 mole fractions, as well as the reactants conversion and H_2 and CO yields. These results are shown in Figures 8 and 9.

Figure 8. (**a**) H_2 and (**b**) CO yields along the length of the reactor, with increasing GHSV [22].

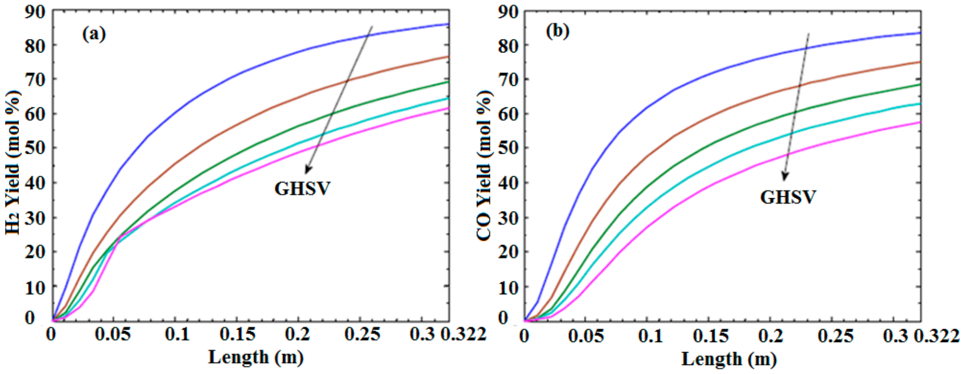

Figure 9. (**a**) H_2 and (**b**) CO yields varying with increasing RED [22].

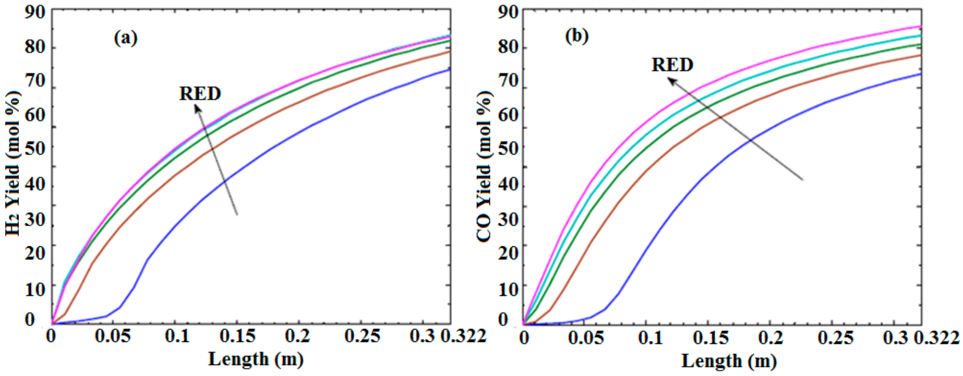

The effect of sulphur addition on the CPOX of ethane over Rh and Pt honeycomb catalysts, was investigated by Cimino *et al.* [23]. Steady state and transient operation of the reactor with poisoning/regeneration cycles were studied. It was observed that sulphur selectively adsorbed on Rh impedes the hydrogenolysis and steam reforming. Sulphur also affects the kinetics of the reverse water gas shift reaction on Rh catalyst operating temperatures less than 750 °C, by increasing the H_2 yield above the equilibrium value. The Pt catalyst is less active for these reactions, but is also more tolerant of sulphur addition. Ballarini *et al.* [24] conducted a study on how composition and preparation method affects the performance of hydrotalcite derived Ru catalysts in the CPOX of methane. They looked at the effect of Ru content, oxidic matrix composition and preparation procedure on the performance of the catalysts. A support catalyst was also established by impregnation on a calcined Mg/Al-CO_3, for comparison purposes. The Ru dispersion and the interaction with the support catalyst decreased with increasing Ru loading and those catalysts which were derived using carbonates showed better performance than those which contained silicates. Catalyst deactivation occurred with increased temperature tests, although with increased Ru loading the initial catalyst activity also increased.

2.3. Filtration Combustion (FC)

The principle of filtration combustion involves an exothermic reaction during fluid motion in a porous matrix. Filtration combustion is significantly different from other homogeneous flames due to two major features: effective heat transfer between solid and gaseous phases, and better diffusion and heat transfer of gaseous phases due to dispersion of reactants and pollutants. Two major types of filtration combustion procedures are adopted in experimental analyses; stationary and transient filtration combustion. In stationary FC, the combustion zone is stabilised within the porous matrix, and transient FC is characterized by a travelling wave where an unsteady combustion front propagates upstream or downstream of the porous matrix. Various studies have aimed at improving an understanding of filtration combustion for syngas production, some of them are discussed in this section.

Smith *et al.* [25] conducted an experimental study on the conversion of Jet-A fuel and butanol to syngas by non-catalytic FC (filtration combustion) in a porous media reactor. The purpose of the study was to explore hydrogen fuel cell usage for portable devices. The experimental setup is shown in Figure 10 and comprises four main sections; the reactor, the fuel vaporisation system, the reactant delivery system and the data acquisition system. The reactor consisted of a Al_2O_3 spheres and alumina insulation (perforated every 2 cm). The air and fuel flow were then varied, according to the equivalence ratio and inlet velocity, and a gas chromatograph was used to analyze the concentration of the various gaseous species present in the syngas. With regards to jet fuel, it found that a maximum of 42% of the hydrogen content was converted to H_2 and 56% of carbon was converted to CO. For butanol, these values were 43% and 72% respectively. Soot production for both fuels exceeded that observed from methane, heptanes and ethanol. The maximum tested equivalence ratio was 3.15, since for values higher than this, the excessive soot production clogged the reactor. With regards to conversion efficiencies, it was found that, contrary to the results obtained through equilibrium calculations, smaller hydrocarbons produced higher syngas yields with jet-fuel having the lowest H_2 and CO yields.

Figure 10. Experimental setup with reactor [25].

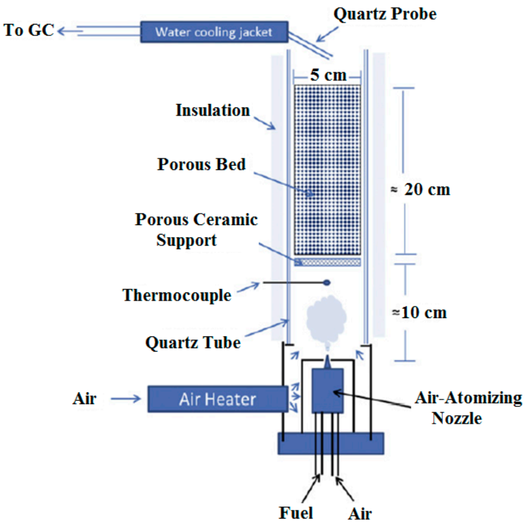

The reburning of NO in ultrarich filtration combustion of methane was analysed by Bingue *et al.* [26]. Transient filtration combustion in inert porous media has the capability to destroy NO_x pollutant emissions. The main components of the experimental setup are the reactor, the flow control system and the diagnostic and data acquisition system. In this case, the reactor is filled with alumina pellets, which serve as the inert porous matrix. The procedure involved initiating an upstream propagating wave, by igniting the mixture at the top of the reactor. The wave travelled downwards and reached the reactor bottom at constant velocity and peak combustion temperature. The mixture composition was then adjusted to initiate a similar downstream propagating wave.

The reburning of NO was studied by adjusting its level in the reactant stream, for a range of equivalence ratios. The results are shown in Figure 11. It was found that two distinct regions of NO_x removal exist, with the addition of NO to the reactant stream, over the range of tested equivalence ratios. In the ultralean regime a small fraction of the NO is oxidized to NO_2 while in the ultrarich regime, a highly efficient NO destruction mechanism is in place which results in more than 60% of the input NO being destroyed.

Figure 11. NO reburning results for various levels of NO addition to the methane/air reactant stream against a range of equivalence ratios [26].

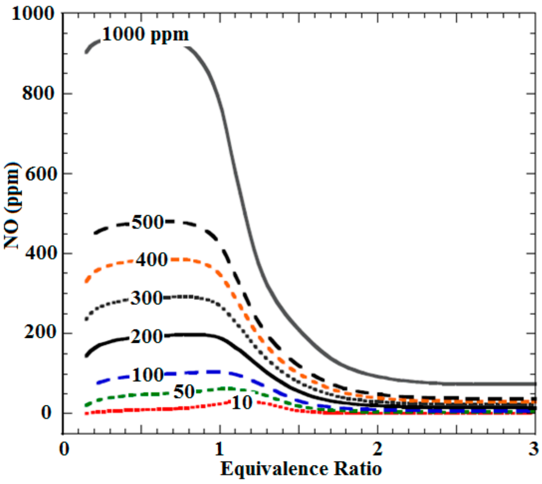

A second study was conducted by Bingue *et al.* [27] on optimizing hydrogen production by transient filtration combustion of methane in inert porous media by oxygen enrichment and depletion was studied. By depleting or enriching the combustion mixture with oxygen, the products of partial oxidation such as H_2 and CO can be controlled. The experimental setup is shown in Figure 12. The reactor is insulated and the inert medium used is a packed bed of Al_2O_3. Methane was introduced at the bottom of the reactor together with varying amounts of air enriched with either nitrogen or oxygen. The equivalence ratios studied were in the range of 1.0 to 3.5.

Figure 12. Experimental setup used in the second experiment by Bingue *et al.* [27].

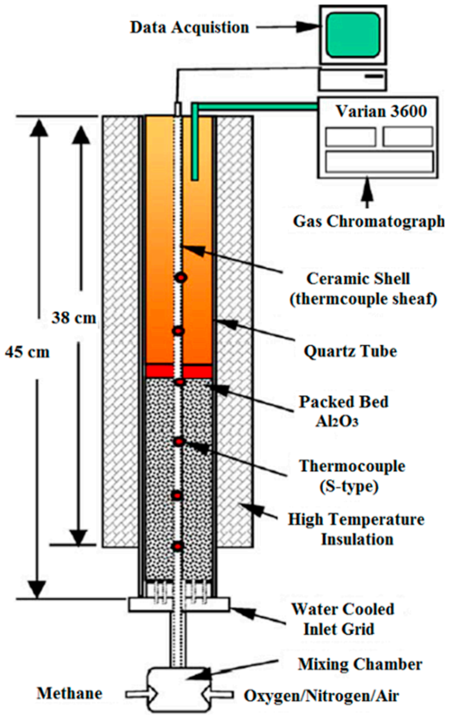

It was found that peak combustion temperatures dropped with oxygen enrichment and the absolute flame propagation rate increased. Three distinct regions of combustion in sequence from rich to ultrarich were identified, and concerning the products of combustion, it was observed that mixtures with higher oxygen in the oxidizer stream generated higher amounts of CO and H_2. These results are shown in Figure 13.

Figure 13. Hydrogen and CO conversion against equivalence ratio, for varying oxygen indices [27].

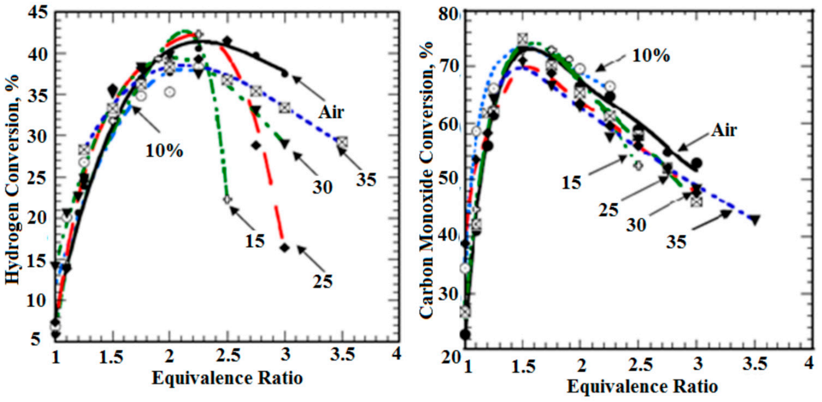

Hydrogen production during ultrarich filtration combustion of various hydrocarbons in porous media was investgated by Toledo *et al.* [28]. The main components of the setup were the reactor (combustion tube), reactant supply system, temperature measurement and gas analyser equipment. The reactor was well insulated to prevent heat loss, and the porous medium used was Al_2O_3 in the form of small spheres. The reactants were premixed and the combustion wave propagation was similar to that which was initiated in the experiment conducted in study by Bingue *et al.* [27], discussed in previous section. The tested equivalence ratios were in the range of 1.0 to 2.0. It was found that complete combustion could not be achieved for rich and ultrarich mixtures due to low oxygen content, and hence products including H_2, CO and C_2 hydrocarbons are formed. The maximum produced hydrogen concentrations were 15%, 14% and 13% for methane, ethane and propane flames respectively. 50% conversion to H_2 was observed and the CO yield was 80% for all fuels. In a study conducted by Dhamrat and Ellzey [29], the conversion of methane to hydrogen using filtration combustion was examined. Both experimental and numerical models were used and compared, and the primary purpose of the study was to understand how various parameters such as inlet velocity of the reactants, equivalence ratio, thermal conductivity and specific heat of the porous matrix affect the conversion efficiency of methane to hydrogen. Ceramic foam was used instead of the typical ceramic beads due to their higher porosity which results in a lower pressure drop.

The tested equivalence ratios were in the range of 1.5 to 5.0. A fixed inlet velocity was maintained while the equivalence ratio was varied. A combustion wave was initiated by igniting a fuel/air mixture and forcing the flame into the porous media by adjusting the equivalence ratio and inlet velocity, which caused the reactor to warm up. The equivalence ratio and inlet velocity were again adjusted to the desired test conditions. Dhamrat and Ellzey [29] also applied a numerical model to validate the results of the experimental procedure and vice versa, and it was found that the numerical model predicted a percentage conversion of approximately 59% while the experimental results showed 73% conversion. Both models predicted that percentage conversion increases with increasing inlet velocity, and that superadiabatic temperatures can be reached. Two regimes of the conversion of methane to hydrogen were observed; partial oxidation (which contributes to the bulk of the final amount of hydrogen produced) and steam reforming. The work of Dhamrat and Ellzey [29] also contributed to the understanding of transient filtration combustion, and the importance of the specific heat and conductivity of the porous medium. A higher specific heat results in a smaller hydrogen yield, and a higher thermal conductivity results in a lower peak temperature and thus a lower conversion efficiency.

The study by Dixon *et al.* [30], on the conversion of liquid heptane to syngas, both numerical and experimental, is also of importance. Filtration combustion in an inert porous medium was used, over a range of equivalence ratios and inlet velocities. The porous medium was a packed bed of alumina. At high equivalence ratios, superadiabatic temperatures were recorded primarily due to the presence of propagating filtration waves. Hydrogen concentration in the products of combustion increased with increasing equivalence ratio and inlet velocity. At equivalence ratios of 2.5 and higher, hydrogen conversion efficiencies as high as 80% were recorded while CO conversion efficiencies peaked at 90%. These results are shown in Figure 14. Minor soot and particulate matter deposition was also recorded. The numerical analysis showed a correlation with the experimental results for equivalence ratios less than 2.0. Aside from showing the importance of the inlet velocity, the study also showed that for heptane based fuel reforming, the optimum equivalence raio lies in the range of 2.5 to 3.5.

Figure 14. H_2 and CO conversion efficiency against equivalence ratio [30].

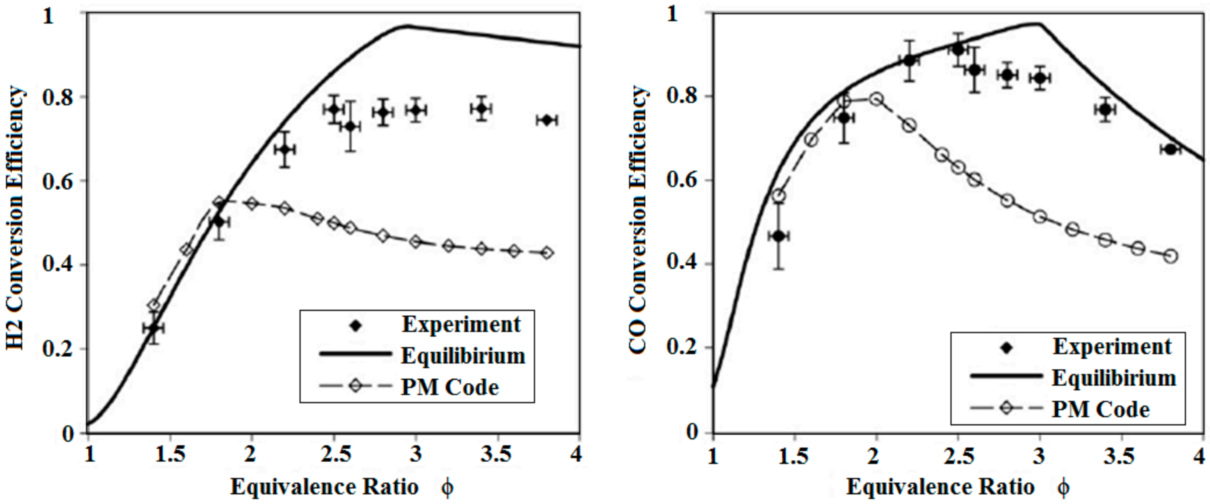

2.4. Autothermal Reforming (ATR)

The basic autothermal reforming mechanism for hydrocarbon fuels involves the following equations:

$$C_nH_m + \frac{x}{2}O_2 \leftrightarrow n\,CO + \frac{m}{2}H_2;\ \Delta H < 0 \quad (3)$$

$$C_nH_m + p\,H_2O \leftrightarrow n\,CO + \left(\frac{m}{2} + n\right)\ H_2 + (p - n)\ H_2O;\ \Delta H > 0 \quad (4)$$

$$CO + H_2O \leftrightarrow CO_2 + H_2;\ \Delta H > 0 \quad (5)$$

The first equation is an exothermic oxidation reaction. The second is an endothermic steam reforming process (steam reforming is discussed in detail in the next section), and the third is a slightly exothermic water-gas-shift reaction. The major benefit of autothermal reforming is that there is no need to supply or dissipate heat to or from the reaction system. This feature has made ATR very interesting and substantial research has been done to investigate its applications, some of which has been discussed in this paper.

A study by Lenz and Aicher [31] investigated the catalytic autothermal reforming of jet fuel. The influence of desulphurization was also examined. The reactor used for the experiment is shown in Figure 15. It consists of three main segments, each with a metallic monolith structure with a wash-coat (Al_2O_3) and Pt and Rh catalysts. The reactor head also consists of a mixing chamber for the reactants. It was concluded that the best reaction efficiency was achieved at a steam to carbon ratio of 1.5 and an air to fuel ratio of 0.28 at a space velocity of GHSV = 50,000 h^{-1}. In the products, the content of alkenes was found to be always higher than that of alkanes. Selective Adsorption for Removing Sulphur (SARS) was found to be the best method of desulphurization.

An experiment similar to that performed by Lenz and Aicher was performed by Pasel *et al.* [32]. A variety of different reactors were used, with Jet A-1 as a fuel. The various reactors and their characteristics are shown in Table 2.

Figure 15. Schematic of reactor [31].

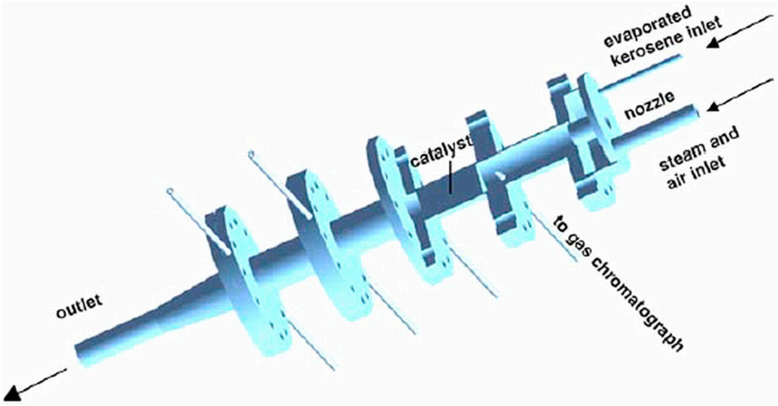

Table 2. Reactors and their characteristics.

Reactor type	Power Class (kW)	Characteristics
ATR 1, ATR 2, ATR 3	0.5–3	Test reformer for catalyst screening Two-fluid nozzle for injection of fuel and air at room temperature External steam generation Designed for PEFC-systems
ATR 4	3	
ATR 5	5	Two fluid nozzle for injection of fuel and air at ambient temperature Internal steam generation Designed for PEFC-systems
ATR 6	5	Single fluid nozzle for fuel injection at room temperature Redesigned fuel evaporation chamber Separate air mixing area Internal steam generation Designed for SOFC-systems
ATR 7	5	Single fluid nozzle for fuel injection at room temperature Design of fuel evaporation chamber from ATR 6 Separate air mixing area Internal steam generation Designed for PEFC-systems
ATR 8	5	Single fluid nozzle for fuel injection at room temperature Slightly modified fuel evaporation chamber Separate air mixing area Internal steam generation Designed for PEFC-systems

The designs for ATR 5, 7, and 8 are shown in Figures 16–18, respectively. It was found that ATR 5 was not suitable for the autothermal reforming of Jet-A1. ATR 7, on the other hand, was found be a suitable reactor as 100% conversion and good stability were exhibited. ATR 8 was found to be even better than ATR 7 as no deposits were formed in its nozzle due to pyrolysis of the fuel. ATR 8 did, however, exhibit a slight decrease in conversion efficiency over time and the efficiency decreased from 100% to 99% towards the end of the experiment *i.e.*, after 2000 h. The primary difference between ATR 7 and ATR 8 is that their fuel evaporation chambers are slightly different.

Figure 16. Schematic of ATR 5 [32].

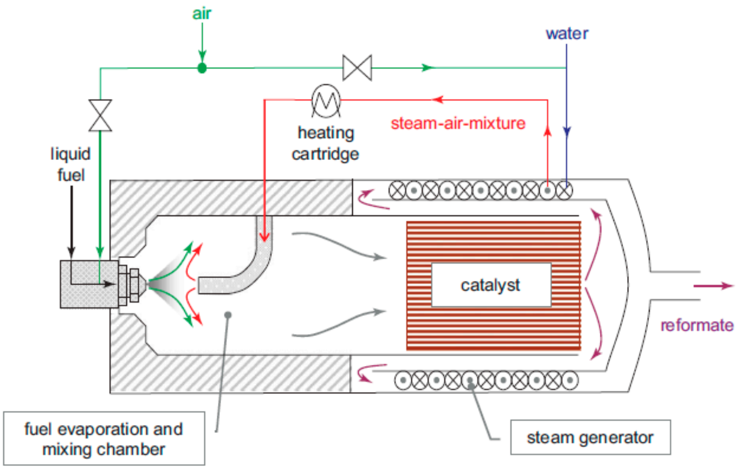

Figure 17. Schematic of ATR 7 [32].

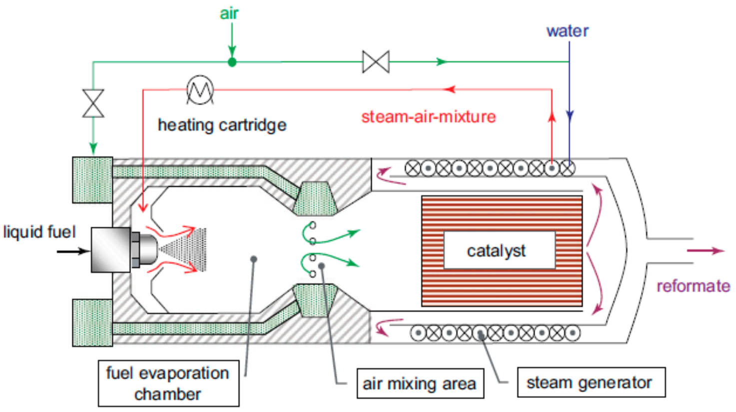

Figure 18. Schematic of ATR 8 [32].

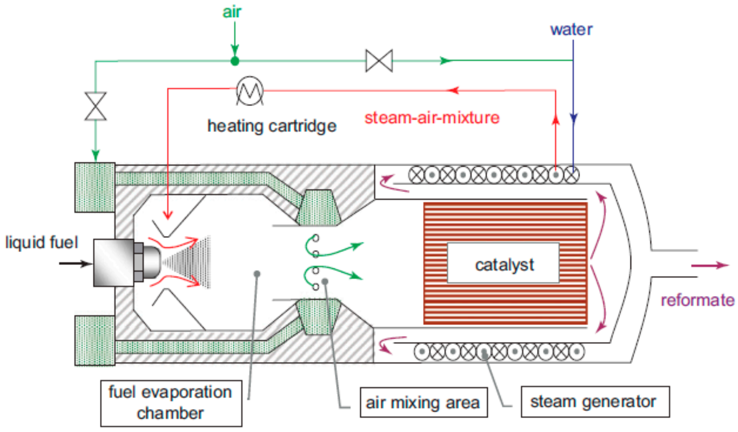

Gökaliler *et al.* [33] conducted a study on hydrogen production by autothermal reforming of LPG for proton exchange membrane fuel cell applications. The purpose of the study was to investigate the performance of a catalyst that could perform well in different compositions of LPG. The mixture chosen for the experiment was 1:1 propane: *n*-butane, and the catalyst was 0.2 weight-percent Pt-15 weight-percent Nickel/δ-Al_2O_3. The effects of temperature, steam/carbon ratio, carbon/oxygen ratio and residence time were investigated, over the temperature range of 623–743K. The results of the showed that the Pt-Ni bi-metallic system is a suitable catalyst for the autothermal reforming of LPG. It was found that hydrogen production rate increases with increasing temperature when no carbon is deposited on the bi-metallic strip. The optimum experimental conditions, under which the highest hydrogen production was achieved, are a steam/carbon ratio of 7.0, a carbon/oxygen ratio of 2.7 and a residence time of 0.51.

Harada *et al.* [34] investigated hydrogen production using autothermal reforming of kerosene. The purpose of the experiment was to analyze the performance of $MgAlO_x$-supported Rhodium catalysts, which possess a physically strong core and support of the surface-concentrated Rh particles with high dispersion. A schematic of the catalyst structure is shown in Figure 19.

Figure 19. Catalyst structure schematic [34].

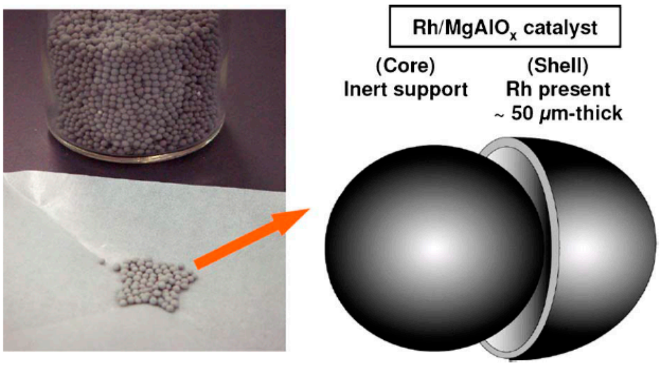

It was found that of all the catalysts tested, those treated in flowing N_2 following impregnation performed the best. The hydrogen production rate achieved was close to the equilibrium value at nearly 60%, the maximum temperature reached was approximately 1200 K at the catalyst bed inlet and decreased towards the exit and reached a value of 1020 K. Paraffin and olefin by-products were low and high hydrogen production was maintained even at an LHSV of 25. The hydrogen production results are shown against N_2 treatment temperature in Figure 20.

Figure 20. N_2 treatment temperature *vs.* H_2 formation rate [34].

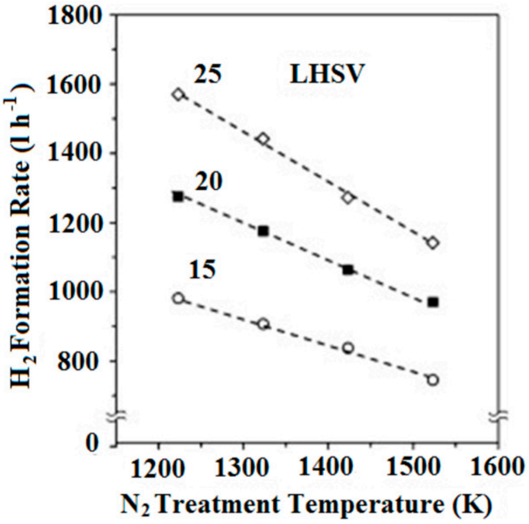

Lai *et al.* [35] performed a study on syngas production through dry ATR from biomass derived gas. A new concept for syngas production was proposed and a parametric study was carried out which investigated the dry ATR process under various CO_2/CH_4 and O_2/CH_4 ratios. The main components of the setup include the reforming unit, reactant supply system, data acquisition system and the gas sampling/analyzing system. The catalyst bed used was of Pt-Rh based noble metals coated over the wash-coat (CeO_2–Al_2O_3) on metallic monolith (Fe–Cr–Al). The conclusions reached by Lai *et al.* were that syngas concentration was affected by both CO_2/CH_4 and O_2/CH_4 molar ratios, coke formation can be avoided in dry ATR if the reaction temperature exceeds 1000 °C, good correlation between the reformate gas temperature, energy loss percentage and equilibrium adiabatic temperature was obtained and methane conversion was dominated by reaction temperature.

Scenna *et al.* [36] performed experiments on autothermal reforming using synthetic JP-8 fuel, which was derived through the Fischer-Tropsch process. The reformate was used to power a solid oxide fuel cell power unit. The reformer unit is shown in Figure 21. The hydrogen production and concentration (dry basis) at various thermal ratings is shown in Figure 22. The JP-8 was successfully reformed at four thermal ratings. The steam to carbon ratio was kept fixed at 2.0. The oxygen to carbon ratio was varied between 0.8 and 1.2. A fuel conversion of greater than 96% was achieved at all fuel equivalency flow rates. The reforming efficiency was 92.2% with hydrogen concentrations up to 36.5%. The results of the experiment showed that coal derived JP-8 can produce high reforming efficiencies while keeping carbon formation to a minimum.

Figure 21. Reactor vessel with cross-sectional (**a**) and longitudinal (**b**) view [36].

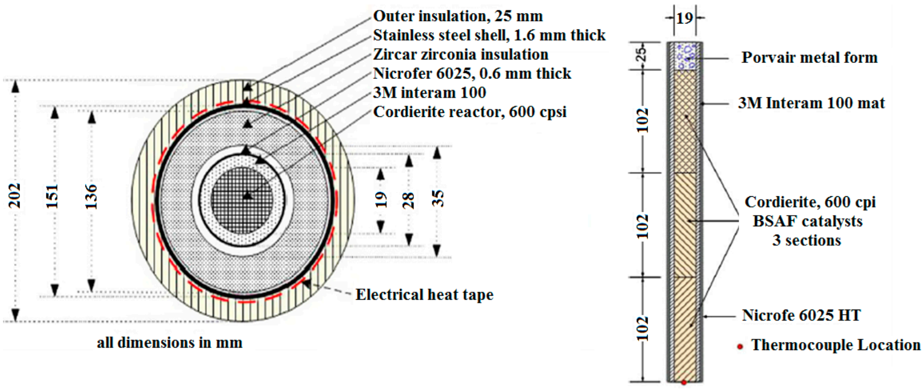

Figure 22. Hydrogen production concentration at various thermal power ratings, and a steam/carbon ratio of 2.0. Open symbols represent concentrations while closed symbols represent flow rates [36].

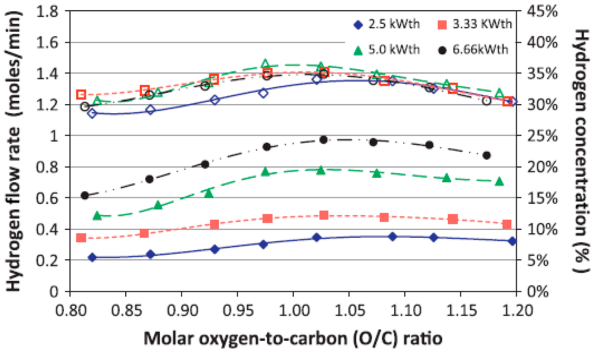

2.5. Steam Reforming

This is the most common method used in industry to produce hydrogen from hydrocarbon fossil fuels. It is an endothermic process where a hydrocarbon, such as methane, is reacted with steam (water) in the presence of a catalyst to produce hydrogen rich syngas. The reaction mechanism follows the set of chemical equations as given below:

$$\mathrm{C_nH_m + nH_2O \rightarrow nCO + \left(\frac{n+m}{2}\right)H_2};\ \Delta H < 0 \tag{6}$$

$$\mathrm{CH_4 + H_2O \leftrightarrow CO + 3H_2};\ \Delta H < 0 \tag{7}$$

$$\mathrm{CO + H_2O \leftrightarrow CO_2 + H_2};\ \Delta H > 0 \tag{8}$$

A significant amount of experimental research has been carried out to investigate the process characteristics of steam reforming, some of which has been discussed in this section.

A parametric study on steam reforming of kerosene over a metal monolithic catalyst, and investigated the influence of preparation conditions and electrical heat testing [37]. A plate-type anodic alumina support was used to prepare a series of Ru catalysts, and their performances in the steam reforming of kerosene were investigated. The alumina support (γ-Al_2O_3/Fe-Cr-Ni alloy/γ-Al_2O_3) is shown in Figure 23.

Figure 23. Anodic alumina support cross-sectional image [37].

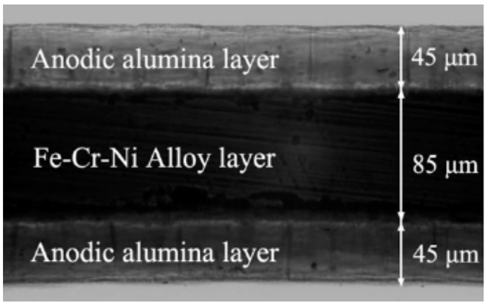

The Ru/Al_2O_3 catalysts were prepared using solution impregnation of the alumina support using ruthenium chloride in deionised water or ethanol solution to improve metal dispersion on the catalyst surface. The samples were dried and their pH levels adjusted using aqueous ammonia. Four types of Ru/Al_2O_3 catalysts were prepared, as well as those loaded with Ce promoter. An electrical heat test was also conducted over the plate type catalyst owing to the high electrical resistance of the Fe–Cr–Ni alloy layer. The setup for this test is shown in Figure 24.

It was found that the catalyst prepared in ethanol solution gave better metal dispersion and durability compared to that prepared in aqueous solution. However, calcination in the air was found to decrease metal dispersion in both aqueous and ethanol solution prepared catalysts. Cerium addition was found to enhance the catalyst tolerance to carbon deposition thereby improving their durability. Furthermore, under an electrical heat test the steam reforming process reached stability after 15 min, which indicates that the start-up time for steam reformer modules can be significantly reduced from 1 to 2 h to a few minutes.

Figure 24. Electrical heat test setup [37].

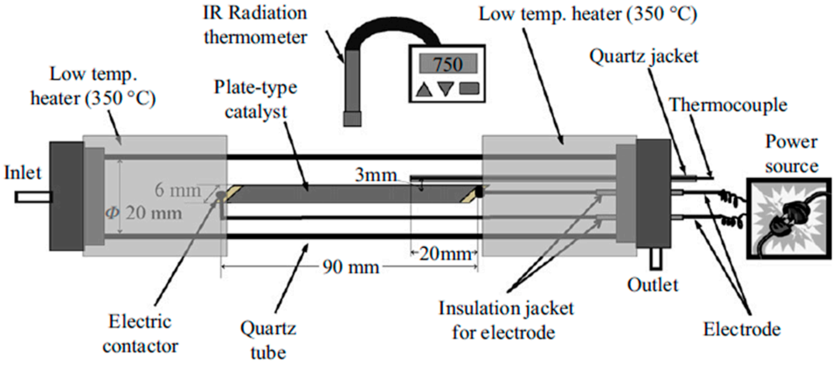

A second similar study by Guo *et al.* [38] investigated the performance of synthesised trace Ru-doped anodic alumina supported Ni catalysts for kerosene steam reforming processes. To prepare the anodic alumina support, a plate type Al/Fe–Cr–Ni alloy/Al clad material was used. An anodic alumina support with an interfacial $NiAl_2O_4$ layer, denoted as $Ni/NiAl_2O_4$, was prepared by repeated impregnation with $Ni(NO_3)_2$. $6H_2O$ aqueous solution and drying, and then calcination. Then, by impregnating the $Ni/NiAl_2O_4$ with a solution of $RuCl_3$, the Ru-doped catalyst, denoted as $Ru\text{-}Ni/NiAl_2O_4$ was prepared. An electrical heating test similar to the previous experiment was also conducted. The synthesised Ru-doped catalyst was found to have good durability during the process and during the electrical heat test the system reached stability in just 15 min and no irregularity was observed during the entire 10 h test. This experiment highlighted the potential of $Ru\text{-}Ni/NiAl_2O_4$ as a suitable catalyst for the steam reforming of kerosene.

Production of hydrogen and syngas through oxidative and steam reforming of biogas, in conventional and micro-reactor systems was studied by Izquierdo *et al.* [39]. The biogas used was synthetic and consisted of 60% CH_4 and 40% CO_2 by volume. The various calcined catalysts used are shown in Table 3. Those which showed good activity and stability were then impregnated in a micro-reactor to investigate process intensification. These were $Ni/Ce\text{–}Zr\text{–}Al_2O_3$ and $Rh\text{-}Ni/Ce\text{–}Al_2O_3$. The micro-reactors showed higher turnover frequencies (TOF) and productivity compared to conventional fixed bed reactors, while similar results were achieved for all the tested catalysts. For the biogas steam reforming process, the lowest hydrogen yield and H_2^{out}/CO^{out} was recorded for the bimetallic $Rh\text{–}Ni/Ce\text{–}Al_2O_3$ and monometallic $Ni/Ce\text{–}Zr\text{–}Al_2O_3$ catalysts. The highest TOF and lowest metal dispersion were achieved using the $Ni/Ce\text{–}Al_2O_3$ catalyst. Furthermore, photochemical characterisation of the catalysts highlighted the importance of morphology and surface properties of the metal phase and its effect on the overall reforming activity.

Miyamoto *et al.* [40] investigated the influence of pre-reforming in steam reforming of dodecane (a main component of kerosene) using a Palladium (Pd) alloy membrane reactor. The Pd membrane was prepared by electroless plating on a porous α-alumina tube. Reaction conditions are shown in Table 4 and the results of hydrogen yield and C1 production are shown in Figure 25.

Table 3. Calcined catalysts used with textural properties and chemical composition [39].

Catalyst	**Surface Area (m^2/g)**	**Pore Volume (cm^3/g)**	**Average Pore Size (Å)**	**Nominal/ICP Measured (wt%)**
Ce–Al support	195.0	0.76	150.1	–
Zr–Al support	180.3	0.67	143.9	–
Ce–Zr–Al support	191.7	0.74	150.7	–
Commercial (composition: 18 wt% NiO)	21.6	0.09	169.5	12.4 (Ni) 0.4 (Ca)
Ni/MgO	25.6	0.13	200.0	20.0/17.2 (Ni)
Ni/Ce–Al_2O_3	163.3	0.59	143.7	13.0/10.8 (Ni) 6.0/3.3 (Ce)
Ni/Zr–Al_2O_3	166.6	0.62	146.3	13.0/11.4 (Ni) 8.0/5.5 (Zr)
Ni/Ce–Zr–Al_2O_3	151.0	0.60	153.2	13.0/10.6 (Ni) 3.0/2.7 (Ce) 4.0/3.6 (Zr)
Rh–Ni/Ce–Al_2O_3	156.8	0.60	150.1	13.0/10.0 (Ni) 1.0/0.9 (Rh) 6.0/3.6 (Ce)

Table 4. Variation of key parameters (reaction temperature, W/F, pressure, catalyst, catalyst amount and S/C) with and without prereforming [40].

Parameters	**With Pre-Reforming**		**Without Pre-Reforming**
	Pre-reformer	**Membrane reformer**	**Membrane reformer**
Reaction temperature (K)	873	773	773
W/F (g cat min/C mol) *	3,000	3,000	6,000
Pressure	Atmospheric pressure		
Catalyst	2% Ru/α-Al_2O_3		
Catalyst amount	5	5	10
S/C	3	3	3

* W/F is the catalyst amount (g)/dodecane molar federate × 12 (C mol/min).

It was found that the pre-reformer had significant effects on the performance of the membrane reactor. With the pre-reformer, the yield exceeded the thermodynamic equilibrium value and deterioration of the conversion and hydrogen yield was not seen. Without the pre-reformer, however, a much lower yield and permeation ratio were recorded. Thus, the importance of pre-reforming was highlighted in this study [40]. A similar fluidised bed membrane reactor was also used by Rakib *et al.* [41] in investigating the steam reforming of propane. The purpose was to investigate an alternate feedstock for the production of hydrogen (syngas). Although there are several methods of producing hydrogen from propane, steam reforming is the most economical. The reaction is given below:

$$C_3H_8 + 3H_2O \rightarrow 3CO + 7H_2; \Delta H = 499 \text{ kJ/mol} \tag{9}$$

During the process certain reactions can take place which result in the production of carbon as an unwanted product. The catalyst chosen for the experiments was commercial RK-212. Equilibrium conditions were nearly achieved in the reactor due to the fast nature of the reactions and the use of permselective membrane panels to remove pure hydrogen shifted the reaction towards complete conversion of the hydrocarbons. The reforming of propane was observed to be limited by the formation of methane, and Rakib *et al.* [41] concluded that a reformer module with membrane panels along the height can be designed for the steam reforming of propane at a moderate temperature range with increased hydrogen yield.

Figure 25. Conversion to C1 products and hydrogen yield at 773 K. Open symbols represent with pre-reforming and closed symbols represent without pre-reforming. Squares represent conversion to C1 and circles represent hydrogen yield [40].

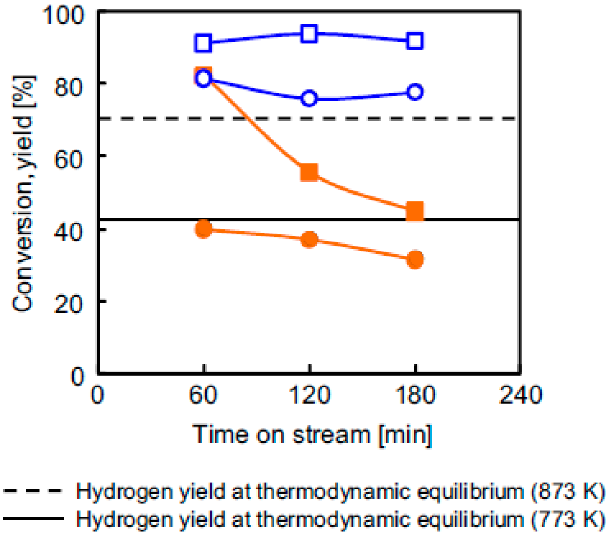

Sahu and Sinha [42] conducted a study on the oxidative steam reforming of vacuum residue for hydrogen production. Vacuum residue is obtained after vacuum distillation of crude petroleum and can, theoretically, be used for hydrogen production. The method proposed in this study consists of two steps. The first step involves reaction of the vacuum residue with ozone to produce oxidized and cracked products. The products of the first step are then subjected to catalytic oxidative steam reforming to produce hydrogen. The catalyst used for this process was ceria and lanthana enhanced alumina support, *i.e.*, La_2O_3–CeO_2–γ-Al_2O_3. It was observed that the catalyst deactivated with time due to coke formation at temperatures higher than 1173 K. The oxidative steam reforming was found to be most efficient at 1173 K and S/C = 4.0 and $O_2/C = 0.5$. The study by Yu *et al.* [43] study looked at hydrogen production steam reforming of kerosene over Ni–La and Ni–La–K/cordierite catalysts. The catalysts were prepared by impregnating cordierite in solutions of $La(NO_3)_3.nH_2O$ and $Ni(NO_3)_2{\cdot}6H_2O$ aqueous solutions, then drying for 3 h at 383 K and finally calcination for 4 h at 773 K. All experiments were conducted in a fixed bed reactor under different conditions. The influence of NiO and La_2O_3 additions on catalyst activity during steam reforming was also investigated. It was found that calcination temperature has a significant effect on the catalyst activity. The catalyst prepared with 5 wt% K_2O, 25 wt% NiO and 10 wt% La_2O_3 was found to give the best performance at a reaction temperature of 773 K.

Table 5 below discusses summarises all the technologies available with their key findings.

Table 5. Summary of Technology Discussed.

Type of Technology	Main Purpose of Study	Key Findings	Source Reference
Thermal Partial Oxidation	The effects of operating conditions such as equivalence ratio and mass flow rate	An air ratio down to 0.4 was the practical limit to perform TPOX of methane; Air pre-heating temperature has no significant effect on the reforming process, but it does affect the soot point; Reactor design seems practical, future modifications could allow it to be incorporated into gas turbine engines	Al-Hammamre *et al.* [8]
Thermal Partial Oxidation	Hydrogen production and soot particulate emissions from rich combustion of methane in an inert porous media based reactor	SiSic is a better porous matrix compared to Al_2O_3 packed bed; Reformer design seems promising, can be incorporated in aircraft gas turbine engines	Loukou *et al.* [9]
Catalytic Partial Oxidation	Catalytic partial oxidation of methane on platinum using spatially resolved profiles	Transportation of the Pt catalyst and the formation of carbonaceous deposits, were responsible for the position of the mechanistic change; The branching ratio between the partial oxidation and complete oxidation reaction were different for the two micro-kinetic models	Korup *et al.* [11]
Catalytic Partial Oxidation	Syngas production through catalytic partial oxidation of methane over lanthanum chromite and lanthanum ferrite perovskites with A-site doping of Ba, Ca, Mg and Sr, for fuel cell applications	A-site doping generally increased the mobility of lattice oxygen ions and therefore decreased the temperature of H_2 and CO production as compared to undoped $LaCrO_3$ and $LaFeO_3$; Both catalysts showed stable performance during the generation-regeneration cycles, but $LaFeO_3$ showed slightly better performance; $(La0.75Sr0.25)FeO_3$ showed the best performance (65% CH_4 conversion, 10% H_2 and 2.8% CO production at 850°C with 100% H_2 selectivity), and is a promising atomic oxygen source for syngas production via catalytic POX of methane	Khine *et al.* [17]
Catalytic Partial Oxidation	Catalytic partial oxidation of n-butanol over LDH derived Ni-based catalysts	The catalysts were proven effective for use in CPOX reactions; Hydrogen production can be increased from 3.76 to 4.01 if O_2 to butanol ratio is increased from 1.5 to 2.0, and the temperature is kept at 700°C	Huang *et al.* [18]
Catalytic Partial Oxidation	Catalytic partial oxidation of methane rich mixtures in non-adiabatic monolith reactors	Radiative heat loss can change the heat release as compared to the adiabatic reactor, and make the reaction more exothermic	Navalho *et al.* [19]
Catalytic Partial Oxidation	Influence of pressure on autothermal catalytic partial oxidation of methane and propane	Below a value of 4 bar, pressure caused an increase in the outlet temperature; In the inlet of the catalyst, pressure had a minimal effect on the reaction kinetics; No change was recorded in the hot spot temperature	Donazzi *et al.* [20]

Table 5. *Cont.*

Type of Technology	Main Purpose of Study	Key Findings	Source Reference
Catalytic Partial Oxidation	Carbon dioxide conversion for syngas production during CPOX of methane	Carbon dioxide conversion for syngas production during CPOX of methane; CO_2 impedes steam reforming and enhances dry reforming. Generally, increasing CO_2 decreases H_2 but increases CO formation; A maximum conversion was obtained at a carbon dioxide to oxygen ratio of 0.2, and with an increasing O/C ratio, the CO_2 conversion decreases	Chen [21]
Catalytic Partial Oxidation	Use of a plasma-assisted gliding arc reactor to model the catalytic partial oxidation of methane to syngas 2D heterogeneous plug-flow radial dispersion and no gradients inside the catalyst pellet	Temperature, reactant conversion and hydrogen and CO yields, showed results which were similar with respect to the simulation and the experimental data; An increase in the GHSV caused a decrease in the reactant conversion and H_2 and CO yields; An increase in the RED resulted in an increase in the CH_4, H_2O and CO_2 mole fractions, as well as the reactants conversion and H_2 and CO yields	Rafiq *et al.* [22]
Catalytic Partial Oxidation	Effect of sulphur addition on the CPOX of ethane over Rh and Pt honeycomb catalysts	Sulphur affects the kinetics of the reverse water gas shift reaction on Rh catalyst operating temperatures less than 750°C, by increasing the H_2 yield above the equilibrium value	Cimino *et al.* [23]
Catalytic Partial Oxidation	How do composition and preparation method affect the performance of hydrotalcite derived Ru catalysts in the CPOX of methane	Ru dispersion and the interaction with the support catalyst decreased with increasing Ru loading and those catalysts which were derived using carbonates showed better performance than those which contained silicates	Ballarini *et al.* [24]
Filtration Combustion	Conversion of Jet-A fuel and butanol to syngas by non-catalytic FC (filtration combustion) in a porous media reactor	Maximum of 42% of the hydrogen content was converted to H_2 and 56% of carbon was converted to CO; For butanol, these values were 43% and 72% respectively Smaller hydrocarbons produced higher syngas yields with jet-fuel having the lowest H_2 and CO yields; Reactor design is robust and can be used in aircraft gas turbine engines	Smith *et al.* [25]
Filtration Combustion	Reburning of NO in ultrarich filtration combustion of methane	Two distinct regions of NOx removal exist with the addition of NO to the reactant stream, over the range of tested equivalence ratios	Bingue *et al.* [26]
Filtration Combustion	Optimizing hydrogen production by transient filtration combustion of methane in inert porous media by oxygen enrichment and depletion	Peak combustion temperatures dropped with oxygen enrichment and the absolute flame propagation rate increased; Three distinct regions of combustion in sequence from rich to ultrarich were identified	Bingue *et al.* [27]

Table 5. *Cont.*

Type of Technology	Main Purpose of Study	Key Findings	Source Reference
Filtration Combustion	Hydrogen production during ultrarich filtration combustion of various hydrocarbons in porous media	Complete combustion could not be achieved for rich and ultrarich mixtures due to low oxygen content, and hence products including H_2, CO and C_2 hydrocarbons are formed; The maximum produced hydrogen concentrations were 15%, 14% and 13% for methane, ethane and propane flames respectively; Fifty per cent conversion to H_2 was observed and the CO yield was 80% for all fuels	Toledo *et al.* [28]
Filtration Combustion	Conversion of methane to hydrogen using filtration combustion	Numerical model predicted a percentage conversion of approximately 59% while the experimental results showed 73% conversion Contributed to the understanding of transient filtration combustion, and the importance of the specific heat and conductivity of the porous medium	Dhamrat and Ellzey [29]
Filtration Combustion	Numerical and experimental conversion of liquid heptane to syngas	At high equivalence ratios, superadiabatic temperatures were recorded At equivalence ratios of 2.5 and higher, hydrogen conversion efficiencies as high as 80% were recorded CO conversion efficiencies peaked at 90%	Dixon *et al.* [30]
Autothermal Reforming	Catalytic autothermal reforming of jet fuel	Best reaction efficiency was achieved at a steam to carbon ratio of 1.5 and an air to fuel ratio of 0.28 at a space velocity of GHSV=50,000h^{-1} In the products, the content of alkenes was found to be always higher than that of alkanes Reactor design unsuitable for gas turbine engines	Lenz and Aicher [31]
Autothermal Reforming	Autothermal reforming of Jet A-1 fuel	ATR 5 was not suitable ATR 7 was a good choice since 100% cinversion efficiency was achieved ATR 8 was even better since no soot was formed Reactor designs are robust and can be used for aircraft gas turbine engines	Pasel *et al.* [32]
Autothermal Reforming	Hydrogen production by autothermal reforming of LPG for proton exchange membrane fuel cell applications	Pt-Ni bi-metallic system is a suitable catalyst for the autothermal reforming of LPG; Hydrogen production rate increases with increasing temperature when no carbon is deposited on the bi-metallic strip; The optimum experimental conditions, under which the highest hydrogen production was achieved, are a steam/carbon ratio of 7.0, a carbon/oxygen ratio of 2.7 and a residence time of 0.51	Gökaliler *et al.* [33]
Autothermal Reforming	Hydrogen production using autothermal reforming of kerosene	Those catalysts treated in flowing N_2 following impregnation performed the best; The hydrogen production rate achieved was close to the equilibrium value at nearly 60%	Harada *et al.* [34]

Table 5. *Cont.*

Type of Technology	Main Purpose of Study	Key Findings	Source Reference
Autothermal Reforming	Syngas production through dry ATR from biomass derived gas	Syngas concentration was affected by both CO_2/CH_4 and O_2/CH_4 molar ratios; Coke formation can be avoided in dry ATR if the reaction temperature exceeds 1000 °C	Lai *et al.* [35]
Autothermal Reforming	Autothermal reforming using synthetic JP-8 fuel, which was derived through the Fischer-Tropsch process	Coal derived JP-8 can produce high reforming efficiencies while keeping carbon formation to a minimum Reformer module has potential for use on aircraft gas turbine engines	Scenna *et al.* [36]
Steam Reforming	Parametric study on the steam reforming of kerosene over a metal monolithic catalyst	The catalyst prepared in ethanol solution gave better metal dispersion and durability compared to that prepared in aqueous solution; Calcination in the air was found to decrease metal dispersion in both aqueous and ethanol solution prepared catalysts	Guo *et al.* [37]
Steam Reforming	Performance of synthesised trace Ru-doped anodic alumina supported Ni catalysts for kerosene steam reforming	Synthesised Ru-doped catalyst was found to have good durability during the process and during the electrical heat test the system reached stability in just 15 min and no irregularity was observed during the entire 10 h test	Guo *et al.* [38]
Steam Reforming	Production of hydrogen and syngas through oxidative and steam reforming of biogas, in conventional and micro-reactor systems	Micro-reactors showed higher turnover frequencies (TOF) and productivity compared to conventional fixed bed reactors, while similar results were achieved for all the tested catalysts	Izquierdo *et al.* [39]
Steam Reforming	Influence of pre-reforming in steam reforming of dodecane (a main component of kerosene) using a Pd alloy membrane reactor	Pre-reformer had significant effects on the performance of the membrane reactor Yield exceeded the thermodynamic equilibrium value and deterioration of the conversion and hydrogen yield was not seen	Miyamoto *et al.* [40]
Steam Reforming	Investigate an alternate feedstock for the production of hydrogen (syngas)	Reformer module with membrane panels along the height can be designed for the steam reforming of propane at a moderate temperature range with increased hydrogen yield	Rakib *et al.* [41]
Steam Reforming	Oxidative steam reforming of vacuum residue for hydrogen production	Catalyst deactivated with time due to coke formation at temperatures higher than 1173 K; The oxidative steam reforming was found to be most efficient at 1173 K and S/C = 4.0 and $O_2/C = 0.5$	Sahu and Sinha [42]
Steam Reforming	Hydrogen production steam reforming of kerosene over Ni–La and Ni–La–K/cordierite catalysts	Calcination temperature has a significant effect on the catalyst activity. The catalyst prepared with 5 wt% K_2O, 25 wt% NiO and 10 wt% La_2O_3 was found to give the best performance at a reaction temperature of 773 K	Yu *et al.* [43]

3. Summary and Future Work

In this paper, a review of hydrogen reforming technologies which hold the potential of improving the performance of aircraft gas turbine engines have been presented. There are five main reforming processes which are currently being worked upon. These are Thermal Partial Oxidation (TPOX), Catalytic Partial Oxidation (CPOX), Autothermal Reforming (ATR), Filtration Combustion (FC) and Steam Reforming (SR).

Each of the above mentioned processes was introduced, and the key reaction mechanisms and kinetics were presented and discussed. Following that, the relevant research work, as available in journal literature, for each type of reforming process was examined. The primary aim of this paper was to present a concise review of all the modern hydrogen reforming techniques and technologies, with the goal of identifying which was the best for application in gas turbine engines.

With regards to TPOX, the main advantages are that the process requires no catalyst, no external heat supply, and no need for additional external feeds such as water or steam. Furthermore, the process is simple, *i.e.*, it requires a simple set-up and can be used with nearly all types of hydrocarbons. The major problem is of hydrogen yield which is generally quite low and substantial soot formation usually occurs. Since the matter at hand requires a high hydrogen yield and lower soot, using a TPOX reformer may not be feasible for use in aircraft engines in its current state. More work needs to be done to increase the hydrogen yield and decreasing soot emissions.

CPOX is another very attractive technology, particularly for small-scale hydrogen production. However, it has been observed in this review, there is very little research which deals with the CPOX of hydrocarbons other than methane. This aspect needs to be worked upon. Furthermore, in several studies, severe coking was observed, which resulted in a decrease in reformer activity. That being said, CPOX of methane is attractive becaus exothermic methane oxidation and endothermic methane formation occur simultaneously during the CPOX reactions, which makes the process very efficient. Before the process can be implemented in aero gas turbine engines, it needs to be further refined and understood.

Steam reforming is a very commonly used reforming process. However, the major drawback is that the process is largely endothermic, which means that an external heat source is required. Coke formation does occur, but Izquierdo *et al.* [39] found that this can be improved with the use of pre-reformer. Although a lot of work has been carried out in the area of steam reforming, the availability of a heat source, as well the pre-reformer, may bring extra complications to the designs of aircraft engines which are to incorporate fuel reformer modules. If he heat of the engine or combustion heat could be used then system based in steam might work, though it would be complicated.

FC is quite different from other reforming processes, primarily because it involves exothermic reactions during fluid motion in a porous media. The main advantages of FC are that there is effective heat transfer between solid and gaseous phases. In addition, it offers better diffusion and heat transfer of gaseous phases due to dispersion of reactants and pollutants. Furthermore, and as has been presented in this review, certain work has aimed at understanding the reaction characteristics during syngas formation using FC, for jet fuels. The main drawback of FC, is the soot formation. Using fuels of high molecular weights, such as jet fuel, can cause soot production. At very high equivalence ratios, the soot has been shown to clog the reactor. Although the set up is slightly more complex compared to processes such as TPOX, reforming efficiencies were achieved. Therefore, FC is a viable option for a reforming process which can be used to produce syngas in aircraft engines, if the issue of soot could be solved. This could be done by various novel technologies including bioabsorption and decomposition. Futher research needs to be done to check this.

ATR is a very interesting process, with a major benefit that there is no need to supply or dissipate heat to or from the reaction. Furthermore, as it has explored in this paper, the setup/apparatus for the reaction is quite simple and can be applied to aircraft engines. Little to no soot formation was observed for most work reviewed in this paper. A significant amount of research is currently being carried out to better understand ATR, and there are numerous studies which have aimed to use jet fuel as the hydrocarbon for ATR processes. Therefore, ATR is a suitable option for a reforming technology which can be used to design aircraft engines with hydrogen reformer modules.

4. Conclusions

The exhaust gases produced by aircraft gas turbine engines, such as CO and NO_x, have been shown to have extremely detrimental effects on the environment, as well as on human health. In an effort to reduce these emissions, the principle of hydrogen reforming has become quite eminent in current combustion research. In applications related to aircraft engines, the principle is that reforming of a hydrocarbon fuel (such as jet fuel) prior to the combustion stage of the gas turbine engine, produces syngas. This contains a large amount of H_2, and is then used as an additive for the remainder of the jet fuel which is ignited in the combustion chamber. In this way, the performance and service-life of aircraft engines can be substantially improved, and their emissions can be reduced.

Over the years, several processes have emerged which can be used for hydrogen reforming, and we have looked at all the major reforming technologies in this review paper. After a thorough examination, it was decided that filtration combustion and autothermal reforming were the two most promising technologies, which could be used for application in reformer modules for aircraft engines. Of course, before they are implemented, further work needs to be conducted on their performance with jet fuel. The effects of service life need to be quantified, and the appropriate reformer modules need to be designed and tested.

Author Contributions

The research was designed by B. Khandelwal. The material for the paper was collated by H. Hassan and B. Khandelwal. The first draft of the paper was written by H. Hassan. The data and content presented therein was analysed and edited by B. Khandelwal. Systematic addition of relevant content was carried out by H. Hassan, with subsequent editing and proofreading done by B. Khandelwal. The final manuscript was organized into its current format by B. Khandelwal. Both authors have read and approved the final manuscript.

Nomenclature

°C, degrees Celsius; CH_4, methane; cm, centimeters; CO, carbon monoxide; CO_2, carbon dioxide; GHSV, gas hourly space velocity; K, Kelvin; LPG, liquiefied petroleum gas; LHSV, liquid hourly space velocity; NO, nitric oxide; NO_X, xxides of nitrogen; ppi, parts per inch; UHC, Unburnt hydrocarbons; wt%, weight percent.

Conflicts of Interest

The authors declare no conflict of interest.

References

1. Juste, G.L. Hydrogen injection as additional fuel in gas turbine combustor. Evaluation of effects. *Int. J. Hydrog. Energy* **2006**, *31*, 2112–2121.
2. Frenillot, J.P.; Cabot, G.; Cazalens, M.; Renou, B.; Boukhalfa, M.A. Impact of H_2 addition on flame stability and pollutant emissions for an atmospheric kerosene/air swirled flame of laboratory scaled gas turbine. *Int. J. Hydrog. Energy* **2009**, *34*, 3930–3944.
3. Khandelwal, B.; Agarwal, K.; Karakurt, A.; Sethi, V.; Singh, R. Preliminary Study of a Novel Gas Turbine Combustor Concept Based on Hydrogen Synthesis from Kerosene Reformation. Presented at 48th AIAA/ASME/SAE/ASEE Joint Propulsion Conference & Exhibit, 30 July–1 August 2012; AIAA: Atlanta, GA, USA, 2009; pp. AIAA-2012-4070.
4. Melo, M.; Sousa, J.M.M.; Levy, Y. Experimental investigation of a novel combustor model for gas turbines. *J. Propuls. Power* **2009**, *25*, 609–617.
5. Melo, M.J.; Sousa, J.M.M.; Costa, M.; Levy, Y. Flow and Combustion Characteristics of a low-NO_x combustor model for gas turbines. *J. Propuls. Power* **2011**, *27*, 1212–1217.
6. Khandelwal, B.; Li, Y.; Murthy, P.; Sethi, V.; Singh, R. Implication of Different Fuel Injector Configurations for Hydrogen Fuelled Micromix Combustors. Presented at ASME 2011 Turbo Expo: Turbine Technical Conference and Exposition, 6–10 June 2011; AIAA: Vancouver, BC, Canada; pp. 293–298.
7. Karakurt, A.; Khandelwal, B.; Sethi, V.; Singh, R. Study of Novel Micromix Combustors to be used in Gas Turbines; using Hydrogen, Hydrogen–Methane, Methane and Kerosene as a fuel. Presented at 48th AIAA/ASME/SAE/ASEE Joint Propulsion Conference & Exhibit, 30 July – 1 August 2012; AIAA: Atlanta, GA, USA, 2012; pp. No. AIAA-2012–4265.
8. Al-Hamamre, Z.; Voß, S.; Trimis, D. Hydrogen production by thermal partial oxidation of hydrocarbon fuels in porous media based reformer. *Int. J. Hydrog. Energy* **2009**, *34*, 827–832.
9. Loukou, A.; Frenzel, I.; Klein, J.; Trimis, D. Experimental study of hydrogen production and soot particulate matter emissions from methane rich-combustion in inert porous media. *Int. J. Hydrog. Energy* **2012**, *37*, 16686–16696.
10. Enger, B.C.; Lødeng, R.; Holmen, A. A review of catalytic partial oxidation of methane to synthesis gas with emphasis on reaction mechanisms over transition metal catalysts. *Appl. Catal. A* **2008**, *346*, 1–27.
11. Korup, O.; Goldsmith, C.F.; Weinberg, G.; Geske, M.; Kandemir, T.; Schlögl, R.; Horn, R. Catalytic partial oxidation of methane on platinum investigated by spatial reactor profiles, spatially resolved spectroscopy, and microkinetic modeling. *J Catal.* **2013**, *297*, 1–16.
12. Quiceno, R.; Perez-Ramirez, J.; Warnatz, J.; Deutschmann, O. Modeling the high temperature catalytic partial oxidation of methane over platinum gauze. *Appl. Catal. A* **2006**, *303*, 166–176.
13. Deutschmann, O.; Koop, J. Detailed surface reaction mechanism for Pt-catalyzed abatement of automotive exhaust gases. *Appl. Catal. B* **2009**, *91*, 47–58.

14. Zerkle, D.K.; Allendorf, M.D.; Wolf, M.; Deutschmann, O. Understanding homogeneous and heterogeneous contributions to the Platinum-catalyzed partial oxidation of ethane in a short-contact-time-reactor. *J. Catal.* **2000**, *196*, 18–39.
15. Mhadeshwar, A.B.; Vlachos, D.G. A catalytic reaction mechanism for methane partial oxidation at short contact times, reforming and combustion and for oxygenate decomposition and oxidation on platinum. *Ind. Eng. Chem.* **2007**, *46*, 5310–5324.
16. Hauptmann, W.; Votsmeier, M.; Vogel, H.; Vlachos, D.G. Modeling the simultaneous oxidation of CO and H_2 on Pt–promoting effect of H_2 on the CO-light-off. *Appl. Catal.* **2011**, *397*, 174–182.
17. Khine, M.S.S.; Chen, L.; Zhang, S.; Lin, J.; Jiang, S.P. Syngas production by catalytic partial oxidation of methane over $(La_{0.7}A_{0.3})BO_3$ (A = Ba, Ca, Mg, Sr, and B = Cr or Fe) perovskite oxides for portable fuel cell applications. *Int. J. Hydrog. Energy* **2013**, *38*, 13300–13308.
18. Huang, L.; Zhou, J.; Hsu, A.T.; Chen, R. Catalytic partial oxidation of *n*-butanol for hydrogen production over LDH-derived Ni-based catalysts. *Int. J. Hydrog. Energy* **2013**, *38*, 14550–14558.
19. Navalho, J.E.P.; Frenzel, I.; Loukou, A.; Pereira, J.M.C.; Trimis, D.; Pereira, J.C.F. Catalytic partial oxidation of methane rich mixtures in non-adiabatic monolith reactors. *Int. J. Hydrog. Energy* **2013**, *38*, 6989–7006.
20. Donazzi, A.; Livio, D.; Diehm, C.; Beretta, A.; Groppi, G.; Forzatti, P. Effect of pressure in the autothermal catalytic partial oxidation of CH_4 and C_3H_8: Spatially resolved temperature and composition profiles. *Appl. Catal. A* **2014**, *469*, 52–64.
21. Chen, W-H. CO_2 Conversion for syngas production in methane catalytic partial oxidation. *J. CO_2 Util.* **2014**, *5*, 1–9.
22. Rafiq, M.H.; Jakobsen, H.A.; Hustad, J.E. Modeling and simulation of catalytic partial oxidation of methane to synthesis gas by using a plasma-assisted gliding arc reactor. *Fuel Process Tech.* **2012**, *101*, 44–57.
23. Cimino, S.; Lisi, L.; Russo, G. Effect of sulphur during the catalytic partial oxidation of ethane over Rh and Pt honeycomb catalysts. *Int. J. Hydrog. Energy* **2012**, *37*, 10680–10689.
24. Ballarini, A.; Benito, P.; Fornasari, G.; Scelza, O.; Vaccari, A. Role of the composition and preparation method in the activity of hydrotalcite-derived Ru catalysts in the catalytic partial oxidation of methane. *Int. J. Hydrog. Energy* **2013**, *38*, 15128–15139.
25. Smith, C.H.; Pineda, D.I.; Zak, C.D.; Ellzey, J.L. Conversion of jet fuel and butanol to syngas by filtration combustion. *Int. J. Hydrog. Energy* **2013**, *38*, 879–889.
26. Bingue, J.P.; Saveliev, A.V.; Kennedy, L.A. NO reburning in ultrarich filtration combustion of methane. *Proc. Combust. Inst.* **2007**, *31*, 3417–3424.
27. Bingue, J.P.; Saveliev, A.V.; Kennedy, L.A. Optimization of hydrogen production by filtration combustion of methane by oxygen enrichment and depletion. *Int. J. Hydrog. Energy* **2004**, *29*, 1365–1370.
28. Toledo, M.; Bubnovich, V.; Saveliev, A.; Kennedy, L. Hydrogen production in ultrarich combustion of hydrocarbon fuels in porous media. *Int. J. Hydrog. Energy* **2009**, *34*, 1818–1827.
29. Dhamrat, R.S.; Ellzey, J.L. Numerical and experimental study of the conversion of methane to hydrogen in a porous media reactor. *Combust. Flame* **2006**, *144*, 698–709.
30. Dixon, M.J.; Schoegl, I.; Hull, C.B.; Ellzey, J.L. Experimental and numerical conversion of liquid heptane to syngas through combustion in porous media. *Combust. Flame.* **2008**, *154*, 217–231.

31. Lenz, B.; Aicher, T. Catalytic autothermal reforming of Jet fuel. *J. Power Sources* **2005**, *149*, 44–52.
32. Pasel, J.; Meißner, J.; Porš, Z.; Samsun, R.C.; Tschauder, A.; Peters, R. Autothermal reforming of commercial Jet A-1 on a scale. *Int. J. Hydrog. Energy* **2007**, *32*, 4847–4858.
33. Gökaliler, F.; Çağlayan, B.S.; Önsan, Z.İ.; Aksoylu, A.E. Hydrogen production by autothermal reforming of LPG for PEM fuel cell applications. *Int. J. Hydrog. Energy* **2008**, *33*, 1383–1391.
34. Harada, M.; Takanabe, K.; Kubota, J.; Domen, K.; Goto, T.; Akiyama, K.; Inoue, Y. Hydrogen production by autothermal reforming of kerosene over $MgAlO_x$-supported Rh catalysts. *Appl. Catal. A* **2009**, *371*, 173–178.
35. Lai, W.-H.; Lai, M.-P.; Horng, R.-F. Study on hydrogen-rich syngas production by dry autothermal reforming from biomass derived gas. *Int. J. Hydrog. Energy* **2012**, *37*, 9619–9629.
36. Scenna, R.; DuBois, T.G.; Nieh, S. Autothermal reforming of synthetic JP-8 derived from a coal syngas stream. *Fuel* **2013**, *108*, 731–739.
37. Guo Y.; Li, H.; Kameyama, H. Steam reforming of kerosene over a metal-monolithic alumina-supported Ru catalyst: Effect of preparation conditions and electrical-heating test. *Chem. Eng. Sci.* **2011**, *66*, 6287–6296.
38. Guo, Y.; Li, H.; Jia, L.; Kameyama, H. Trace Ru-doped anodic alumina-supported Ni catalysts for steam reforming of kerosene: Activity performance and electrical-heating possibility. *Fuel Process. Tech.* **2011**, *92*, 2341–2347.
39. Izquierdo, U.; Barrio, V.L.; Lago, N.; Requies, J.; Cambra, J.F.; Güemez, M.B.; Arias, P.L. Biogas steam and oxidative reforming processes for synthesis gas and hydrogen production in conventional and microreactor reaction systems. *Int. J. Hydrog. Energy* **2012**, *37*, 13829–13842.
40. Miyamoto, M.; Hayakawa, C.; Kamata, K.; Arakawa, M.; Uemiya, S. Influence of the pre-reformer in steam reforming of dodecane using a Pd alloy membrane reactor. *Int. J. Hydrog. Energy* **2011**, *36*, 7771–7775.
41. Rakib, M.A.; Grace, J.R.; Lim, C.J.; Elnashaie, S.S.E.H.; Ghiasi, B. Steam reforming of propane in a fluidized bed membrane reactor for hydrogen production. *Int. J. Hydrog. Energy* **2010**, *35*, 6276–6290.
42. Sahu, M.K.; Sinha, A.S.K. Oxidative steam reforming of vacuum residue for hydrogen production. *Int. J. Hydrog. Energy* **2012**, *37*, 1425–1435.
43. Yu, X.; Zhang, S.; Wang, L.; Jiang, Q.; Li, S.; Tao, Z. Hydrogen production from steam reforming of kerosene over Ni–La and Ni–La–K/cordierite catalysts. *Fuel* **2006**, *85*, 1708–1713.